Continuum approach to car-following models

Peter Berg,[1,*] Anthony Mason,[2] and Andrew Woods[1,†]
[1]*School of Mathematics, University of Bristol, Bristol BS8 1TW, United Kingdom*
[2]*Department of Applied Mathematics and Theoretical Physics, University of Cambridge, Cambridge CB3 9EW, United Kingdom*
(Received 6 July 1999)

A continuum version of the car-following Bando model is developed using a series expansion of the headway in terms of the density. This continuum model obeys the same stability criterion as its discrete counterpart. To compare both models we show that traveling wave solutions of the Bando model are very similar to those of the continuum model in the limit of small changes of headway. As the change of headway across the wave increases the solutions gradually diverge. Our transformation relating headway to density enables predictions of the global impact and characteristics of any car-following model using the analogous continuum model. In contrast, we show that the conventional continuum models which account for effects of pressure and dispersion predict behavior which is distinct from the global behavior of discrete models.

PACS number(s): 89.40.+k, 45.70.Vn, 02.60.Cb

I. INTRODUCTION

The purpose of this work is to develop a systematic method for relating car-following and continuum models of road traffic. The relation between these models is of interest since they provide different pictures of the flow, which should converge in the appropriate limit. Continuum models give an overview of the global traffic flow, which is important for developing insight into traffic quantities such as throughput, density distributions, or the onset of jams, without detailed regard to the properties of each car. They can illustrate the effects of speed control systems along the road and allow for analytical calculations. Continuum models differ from car-following models with regard to carrying out simulations. With continuum models one has to deal with two coupled partial differential equations instead of a few hundred or even thousands of ordinary differential equations in the latter case.

Car-following models represent the only class of models that describes each vehicle in a deterministic manner including the response to local variables such as speed, headway, and change of headway. Therefore they seem to be of great importance with regard to autonomous cruise control systems (ACCS), which should stabilize the flow as well as maximize the throughput. In this paper we follow the Bando model [1] of road traffic, in which the acceleration of every car is determined by its velocity v_n and a desired speed $V(b_n)$ depending on the headway b_n to the car in front

$$\dot{v}_n = a[V_B(b_n) - v_n]. \tag{1}$$

$V_B(b_n) = \tanh(b_n - 2) - \tanh(-2)$ is called the optimal velocity (OV) function and a is the driver's sensitivity, which equals the inverse of the reaction time, say T. This model is able to reproduce various features of road traffic and is the subject of much current research [2–4]. By developing a formal asymptotic procedure we derive the continuum approximation of the car following model, which is valid when the spacing between cars is small relative to the length scale of changes in speed and headway. We then compare this with the continuum model of Kerner and Konhäuser [5] proposed in the literature.

Continuum models have become progressively more complex incorporating effects of inertia and dispersion. Usually one has to deal with two coupled differential equations in terms of the density ρ and the velocity v of the cars in space and time. Besides the equation for the conservation of cars (continuity equation)

$$\rho_t + (v\rho)_x = 0 \tag{2}$$

the system evolves according to a dynamic equation, which describes the acceleration of cars depending on some local traffic quantities. A typical model is the Kerner-Konhäuser model

$$v_t + v v_x = \frac{V_{KK}(\rho) - v}{\tau} - c_0^2 \frac{\rho_x}{\rho} + \mu \frac{v_{xx}}{\rho} \tag{3}$$

with an optimal velocity function $V_{KK}(\rho)$. The coefficients c_0^2 of the ''pressure'' term and μ of the ''viscosity'' (dispersive) term, respectively, are considered to be constant. This model is able to describe the formation of instabilities and traffic jams. In discussions [6] of the derivation of the higher order terms, it appears that the diffusion term was originally introduced as a means of stopping steepening waves forming discontinuous shocks. Nagel [7] explained the diffusion term as an averaging effect caused by implicit random fluctuations in ρ and v. It has been argued that these noise terms are important, since they can have a profound effect on solutions of certain PDE's. For instance, Burger's equation

$$u_t + u u_x = \lambda u_{xx} \tag{4}$$

has well-known traveling N-wave solutions which cease to exist if Gaussian noise is added to the right-hand side. Here, rather than these heuristically motivated continuum models, we aim to derive an asymptotic equation analogous to Eq. (3) from the car-following model. We thereby establish that such

*Electronic address: Peter.Berg@bris.ac.uk
†Electronic address: A.W.Woods@bris.ac.uk

diffusive behavior is an implicit part of the car-following model. In the case of a homogeneous, stationary flow all time and space derivatives vanish, and for the car-following model we then obtain the relation between speed v_0 and headway b_0

$$v_0 = V_B(b_0), \tag{5}$$

while from the continuum model we have

$$v_0 = V_{KK}(\rho_0). \tag{6}$$

For such uniform flow conditions, the density is simply given by the inverse of the headway

$$\rho = 1/b, \tag{7}$$

and one can compare both types of model by drawing a *fundamental diagram* that describes the dependence of the flow q_0 (throughput) on the headway (car-following model)

$$q_0(b_0) = \frac{v_0}{b_0} = \frac{V_B(b_0)}{b_0} \tag{8}$$

$$\Rightarrow q_0(\rho_0) = V_B(1/\rho_0)\rho_0 \tag{9}$$

or density (continuum model)

$$q_0(\rho_0) = V_{KK}(\rho_0)\rho_0. \tag{10}$$

In nonhomogeneous, nonstationary situations the car-following and continuum models can only be compared by stability analysis and numerical simulations. It is hard to say which terms or effects are responsible for the difference in the simulations. Here we show that the relation between headway and density is of great importance. When there are long range fluctuations in the headway or the density along the road, the usual definition of the density in terms of the headway (7) is only an approximation. In Sec. II we introduce a more accurate method to relate these variables.

II. DERIVATION OF THE CONTINUUM MODEL

The difficulty of relating car-following and continuum models of road traffic is in part a result of the fact that the first is based on the headway and the latter on the vehicle density. It is important to relate these two quantities correctly. In the literature the density ρ is usually defined as the inverse of headway (7). There is a problem with this definition. For instance, suppose we have a set of cars positioned at $x = 1,2,4,8, \ldots$. The car at position x has headway $b = x$. Using formula (7), we obtain $\rho = 1/x$, which is extended into continuum domain by permitting x to take any positive, real value. According to this, the number of cars on the open interval (1,y) is $\log_e y$. However the actual answer is $\log_2 y$ and so we are consistently a factor of $\log_e 2$ wrong.

We deduce that for nonhomogeneous flow situations we cannot transform the car-following model simply using relation (7). We need a consistent way to set up a map

$$\{x_i\} \mapsto [\rho : \mathbb{R} \mapsto \mathbb{R}], \tag{11}$$

where the set $\{x_i\}$ represents the positions of the vehicles at a given instant in time, and $\rho(x)$ is the associated density function from which we should be able to find the positions of the vehicles. One approach is to require that

$$\int_{x_i}^{x_{i+1}} \rho(x)dx = 1 \tag{12}$$

for all i. Thus in addition to our density function, we require the position of car 1. Given only the condition (12), map (11) is not unique, but its inverse is. However, it is the inverse map that we require in constructing a continuum equation of motion from a car-following law. We use the definition of headway $b = x_{i+1} - x_i$ to arrive at an equation involving the continuum variable ρ by extending Eq. (12) to all points along the road

$$\int_x^{x+b(x,t)} \rho(x',t)dx' = \int_0^{b(x,t)} \rho(x+y,t)dy \equiv 1. \tag{13}$$

Expanding the second integral in powers of y, we integrate to obtain the asymptotic series [8]

$$b\rho + \frac{1}{2!}b^2\rho_x + \frac{1}{3!}b^3\rho_{xx} + \cdots = 1. \tag{14}$$

The first term corresponds to the usual definition of the density (7). We expand the series to this order for two reasons. First, we would like to obtain a continuum model that is capable of describing some characteristic traffic parameters mentioned by Kerner and Konhäuser [5]. They showed that a dispersive term has to be incorporated to do so. Second, these higher order terms are needed to maintain the same stability criterion for the continuum model as for the car-following model, as we show in Sec. III.

It is assumed that each term is of smaller magnitude than the one preceding it. This assumption is at the core of continuum approximations of many kinds, and can be summarized by condition

$$\epsilon_\Lambda = \frac{\Lambda_x}{\Lambda} \ll 1 \tag{15}$$

for all scalar quantities Λ associated with traffic. It amounts to saying that changes in the flow occur over a length scale of many vehicles. However, even in this case the continuum approach is not applicable to sharp fronts.

If we consider the cubic term to be much smaller than the linear and quadratic term, we can first solve the quadratic equation for b. We obtain

$$b \approx \frac{1}{\rho} - \frac{\rho_x}{2\rho^3}. \tag{16}$$

Regarding the cubic term as a perturbation, we expand b in a perturbation series and approximate the solution as

$$b \sim \frac{1}{\rho} - \frac{\rho_x}{2\rho^3} - \frac{\rho_{xx}}{6\rho^4} + \frac{\rho_x^2}{2\rho^5} + \cdots. \tag{17}$$

The first term represents the classic transformation for relating the headway and the density. The second term is similar to a *pressure term* in gas kinetics and acts to destabilize the

traffic flow. If we only retain this term, then the continuum model is always unstable unlike real traffic flow. The dispersive term ρ_{xx} smoothes variations in traffic density and has a stabilizing effect on traffic flow, which counteracts the pressure term. We therefore retain terms up to this order.

Equation (17) can then be substituted into car-following models to yield equations for ρ instead of b.

So far we have established a link between the continuum density and the headway. The other quantity relevant to both continuum and car-following models is the speed v. In order to link the two models completely, we need to establish that now v is consistent with the quantity representing the speed of each vehicle in the car-following models.

Taking a total time derivative of each side of Eq. (13), we obtain

$$\int_x^{x+b} \rho_t(y,t)dy + (x_t + b_t)\rho(x+b,t) - x_t\rho(x,t) \tag{18}$$

$$= \int_x^{x+b} \rho_t(y,t)dy + v(x+b,t)\rho(x+b,t) - v(x,t)\rho(x,t) \tag{19}$$

$$= \int_x^{x+b} [\rho_t(y,t) + (\rho(y,t)v(y,t))_y]dy \tag{20}$$

$$= 0. \tag{21}$$

Hence the conservation equation

$$\rho_t + (\rho v)_x = 0 \tag{22}$$

guarantees that the integral of density along the road from any vehicle to the vehicle it is following is 1, so in this sense, the definition of velocity v is consistent.

Applying our analysis to the second-order model of Bando *et al.* [1] in Eq. (1), we obtain the expression for the conservation of cars (22), coupled with the approximation of the car-following model

$$v_t + v v_x = a[\overline{V}(\rho) - v] + a\overline{V}'(\rho)\left[\frac{\rho_x}{2\rho} + \frac{\rho_{xx}}{6\rho^2} - \frac{\rho_x^2}{2\rho^3}\right]. \tag{23}$$

Here we have set

$$\overline{V}(\rho) = V_B(1/\rho), \tag{24}$$

$$0 < \frac{\partial V_B(b)}{\partial b}\Big|_{b=1/\rho} = -\rho^2 \frac{\partial \overline{V}(\rho)}{\partial \rho} = -\rho^2 \overline{V}'(\rho). \tag{25}$$

Equation (23) is analogous to the Kerner-Konhäuser model (3). However, an important difference between that model and the new model (23) lies in the coefficients of the higher order terms. In the Kerner-Konhäuser model the coefficients are assumed to be constant, while expression (23) reveals that they actually depend on ρ. c_0^2 is now analogous to the term $-[a\overline{V}'(\rho)/2]$. By comparison with the discrete Bando model numerical simulations show that the dependence of these coefficients on the density ρ is necessary to match the length scale and qualitative behavior of shock wave solutions (Sec. V). The accuracy increases with further terms of the asymptotic series (17).

Nagel [7] argues that the diffusion term can be regarded as stochasticity added as a high-frequency correction to density, which is supposed to be slowly varying in space and time. However, our analysis reveals that the transformation from a car-following to a continuum model also produces a diffusive or smoothing effect, without the need to introduce any stochasticity.

III. STABILITY ANALYSIS

Before proceeding with numerical calculations, we first show that the continuum version of the Bando model (22), (23) obeys the same stability criterion as its discrete counterpart. Bando *et al.* [1] proved that an initially homogeneous flow is unstable, if the relation

$$\frac{2V_B'(b_0)}{a} > 1 \tag{26}$$

between the driver's sensitivity a and the derivative of the OV function V_B' at the given value of $\rho_0 = 1/b_0$ is satisfied. The analogous criterion for the continuum model may be found by linearizing the model

$$\rho_t + (\rho v)_x = 0, \tag{27}$$

$$v_t + v v_x = a[\overline{V}(\rho) - v] + a\overline{V}'(\rho)\left[\frac{\rho_x}{2\rho} + \frac{\rho_{xx}}{6\rho^2} - \frac{\rho_x^2}{2\rho^3}\right] \tag{28}$$

around some initial values ρ_0 and $v_0 = \overline{V}(\rho_0)$

$$\rho = \rho_0 + \hat{\rho}, \tag{29}$$

$$v = v_0 + \hat{v}. \tag{30}$$

This leads to the perturbation equations

$$\hat{\rho}_t + \rho_0 \hat{v}_x + v_0 \hat{\rho}_x = 0, \tag{31}$$

$$\hat{v}_t + v_0 \hat{v}_x = a[\overline{V}'(\rho_0)\hat{\rho} - \hat{v}] + a\overline{V}'(\rho_0)\left[\frac{\hat{\rho}_x}{2\rho_0} + \frac{\hat{\rho}_{xx}}{6\rho_0^2}\right]. \tag{32}$$

We now calculate the eigenvalues $\omega(k)$ of a harmonic disturbance

$$\vec{f}(x,t) = \begin{pmatrix} \hat{\rho}(x,t) \\ \hat{v}(x,t) \end{pmatrix} = \begin{pmatrix} \hat{\rho}_0 \\ \hat{v}_0 \end{pmatrix} \exp\{i[kx - \omega(k)t]\}, \tag{33}$$

so that we can rewrite the equations in the form

$$\begin{pmatrix} i(kv_0-\omega) & ik\rho_0 \\ -a\overline{V}'-\dfrac{ia\overline{V}'k}{2\rho_0}+\dfrac{a\overline{V}'k^2}{6\rho_0^2} & i(kv_0-\omega)+a \end{pmatrix} \times \begin{pmatrix} \hat{\rho}_0 \\ \hat{v}_0 \end{pmatrix} \exp\{i[kx-\omega(k)t]\}=0. \quad (34)$$

This equation has nontrivial solutions if the determinant vanishes

$$\begin{vmatrix} i(kv_0-\omega) & ik\rho_0 \\ -a\overline{V}'-\dfrac{ia\overline{V}'k}{2\rho_0}+\dfrac{a\overline{V}'k^2}{6\rho_0^2} & i(kv_0-\omega)+a \end{vmatrix}=0. \quad (35)$$

As long as the imaginary part of ω is negative, the system is stable. Solutions have the form

$$\omega_{1,2}(k)=kv_0-i\frac{a}{2} \times\left[1\pm\sqrt{1+\frac{2\overline{V}'}{a}\left(k^2-i2\rho_0k+\frac{i}{3\rho_0}k^3\right)}\right], \quad (36)$$

and by defining

$$\Omega(k):=\mathrm{Re}\left[1+\frac{2\overline{V}'}{a}\left(k^2-i2\rho_0k+\frac{i}{3\rho_0}k^3\right)\right]^{1/2} \quad (37)$$

the criterion is equivalent to $|\Omega(k)|<1$. By writing

$$|\Omega(k)|=\left[\left(1+\frac{2\overline{V}'}{a}k^2\right)^2+\left(-\frac{4\overline{V}'\rho_0}{a}k+\frac{2\overline{V}'}{3a\rho_0}k^3\right)^2\right]^{1/4}|\cos(\phi/2)| \quad (38)$$

$$=\left[\left(1+\frac{2\overline{V}'}{a}k^2\right)^2+\left(-\frac{4\overline{V}'\rho_0}{a}k+\frac{2\overline{V}'}{3a\rho_0}k^3\right)^2\right]^{1/4}\frac{\sqrt{1+\cos\phi}}{\sqrt{2}}, \quad (39)$$

where

$$\phi=\arg\left[1+\frac{2\overline{V}'}{a}\left(k^2-i2\rho_0k+\frac{i}{3\rho_0}k^3\right)\right], \quad (40)$$

it may be seen that the condition $\mathrm{Im}(\omega)<0$ is equivalent to

$$\left[\left(1+\frac{2\overline{V}'}{a}k^2\right)^2+\left(-\frac{4\overline{V}'\rho_0}{a}k+\frac{2\overline{V}'}{3a\rho_0}k^3\right)^2\right]^{1/4}\frac{1}{\sqrt{2}}\sqrt{1+\frac{1+(2\hat{V}'/a)k^2}{\left[\left(1+\frac{2\overline{V}'}{a}k^2\right)^2+\left(-\frac{4\overline{V}'\rho_0}{a}k+\frac{2\overline{V}'}{3a\rho_0}k^3\right)^2\right]^{1/2}}}<1. \quad (41)$$

In order to solve this inequality, we restrict k to be nonnegative, since $|\Omega(k)|$ is symmetric. Solving $|\Omega(k)|=1$ leads to three solutions

$$k_0=0,\quad k_\pm=\sqrt{6\rho_0^2\pm\frac{3a\rho_0}{\overline{V}'}\sqrt{-\frac{2\overline{V}'}{a}}}. \quad (42)$$

Recall that $\overline{V}'<0$ from Eq. (25). k_- is always real, whereas k_+ might be either real or complex. Since we know that $|k_+|<k_-$, $\Omega(0)=1$ and

$$\Omega(k)\overset{k\to\infty}{\to}-\infty, \quad (43)$$

we can deduce from the continuity of $\Omega(k)$ that $\Omega(k_-)=-1$. So for $k>k_-$ the model is unstable, but since this corresponds to disturbances which are smaller than the initial headway, we do not take this case into further consideration. However, if k_+ is real, there is a region $0<k<k_+$ of instability $\Omega(k)>1$ with respect to long wavelengths. If $k_+\notin\mathbb{R}$, which means

$$6\rho_0^2+\frac{3a\rho_0}{\overline{V}'}\sqrt{-\frac{2\overline{V}'}{a}}<0, \quad (44)$$

the system is stable. Taking $V_B'=-\rho_0^2\overline{V}'$ into account, this reduces to

$$\frac{a}{2V_B'}>1, \quad (45)$$

which is exactly the stability criterion found by Bando *et al.* [cf. Eq. (26)]. This model is unstable in a regime $0<\rho_{c_1}^B<\rho<\rho_{c_2}^B$ such that

$$\frac{a}{2\ V_B'(1/\rho)}<1. \quad (46)$$

A stability analysis for the Kerner-Konhäuser model leads to a criterion similar to Eq. (38). Now the system is stable, if

$$|\Omega_{KK}(k)|=\left|\mathrm{Re}\left[1+\frac{i4\rho_0aV_{KK}'k-4\rho_o^2c_0^2k^2}{(a\rho_0+\mu k^2)^2}\right]^{1/2}\right|<1 \quad (47)$$

is satisfied. Taking the limits

$$k\to0:|\Omega(k)_{KK}|\to1-\frac{2c_0^2}{a^2}k^2\to1_-, \quad (48)$$

$$k\to\infty:|\Omega(k)_{KK}|\to\sqrt{1-\frac{4\rho_0^2c_0^2}{\mu k^2}}\to 1_-. \tag{49}$$

This shows that the model is stable for any initial value ρ_0 of the density and arbitrary sensitivity $a=1/T$ with respect to short and long range disturbances unlike the continuum analog of the Bando model. However, for the set of parameters chosen [see Eqs. (79)–(85)], the model is unstable in an intermediate range $0<\rho_{c_1}^{KK}<\rho<\rho_{c_2}^{KK}$ in an analogous way to the Bando model but $\rho_{c_1}^{KK}\neq\rho_{c_1}^{B}$ and $\rho_{c_2}^{KK}\neq\rho_{c_2}^{B}$. This explains the basic difference between these two continuum models.

IV. COMPARISON OF TRAVELING WAVE SOLUTIONS

To test the accuracy of our model, we compare some traveling wave solutions of the car-following Bando model in the stable regime [9] with those of the continuum version.

The traveling wave of speed c has the form

$$v(x,t)=v(x-ct)=v(z), \tag{50}$$

$$\rho(x,t)=\rho(x-ct)=\rho(z), \tag{51}$$

$$z=x-ct, \tag{52}$$

where the equation for the conservation of cars (22) yields the relation

$$\rho(v-c)=q_0. \tag{53}$$

q_0 is some integration constant that is determined by the boundary conditions $\rho_-=\rho(x\to-\infty)$, $\rho_+=\rho(x\to\infty)$, $v_-=v(x\to-\infty)$, and $v_+=v(x\to\infty)$, respectively, as follows:

$$q_0=\rho_+(v_+-c) \tag{54}$$

$$=\rho_+[\overline{V}(\rho_+)-c] \tag{55}$$

$$=\rho_-(v_--c) \tag{56}$$

$$=\rho_-[\overline{V}(\rho_-)-c]. \tag{57}$$

Equations (54)–(57) determine that the wave speed c has value

$$c=\frac{\rho_+\overline{V}(\rho_+)-\rho_-\overline{V}(\rho_-)}{\rho_+-\rho_-} \tag{58}$$

and so both the variables q_0 and c are uniquely determined by the values of ρ at $\pm\infty$. If we substitute these relations into our model equation (23) and make the following transformation

$$u(z)=v(z)-c, \tag{59}$$

we obtain the equation for the speed of cars u in the frame moving with the wave in the form

$$uu_z=a[\overline{V}(q_0/u)-u-c]-a\overline{V}'(q_0/u)\left(\frac{u_z}{2u}+\frac{u_{zz}}{6q_0}+\frac{2u_z^2}{3q_0u}\right). \tag{60}$$

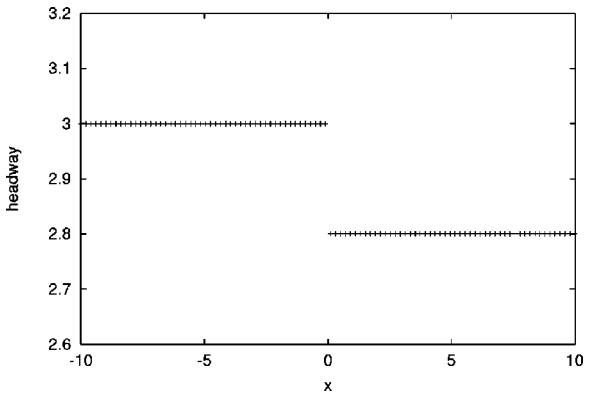

FIG. 1. Initial change of headway in the Bando model, $t=0$.

Throughout the remaining parts we assume $a=2.0$ in order to be in the stable regime. The wave that develops from the initial condition shown in Fig. 1 is shown in Fig. 2 evolving towards the wave solution of the continuum model (60). As the initial jump in headway increases, the wave develops an oscillatory tail. Because of the increasing of headway gradients, the solution governed by the continuum model begins to diverge from its discrete car-following counterpart, although the length scale and the oscillatory characteristic of the wave are still described properly (Fig. 3).

If the downstream headway in the car-following model is decreased below some critical value $\rho_+=\rho_{bw}$, an unusual type of nonlinear wave solution develops [9], [10]. It consists of two traveling waves of different speed, separated by a growing region of congested traffic of density ρ_{gap}. We may call this a Bando wave. Given ρ_{gap}, which can only be determined numerically, we can calculate traveling wave solutions in the analogous continuum model for both up- and downstream propagating shocks. They may be matched together to describe the unusual wave type, if one knows the long-time behavior of the gapwidth. We assume that in this limit the gap will increase at a constant rate v_{gap} which can be calculated from the continuum model according to

$$v_{gap}=c_{down}-c_{up}. \tag{61}$$

Here c_{down} and c_{up} represent the downstream and the upstream wave velocity, respectively. Both parameters can be determined following Eq. (58)

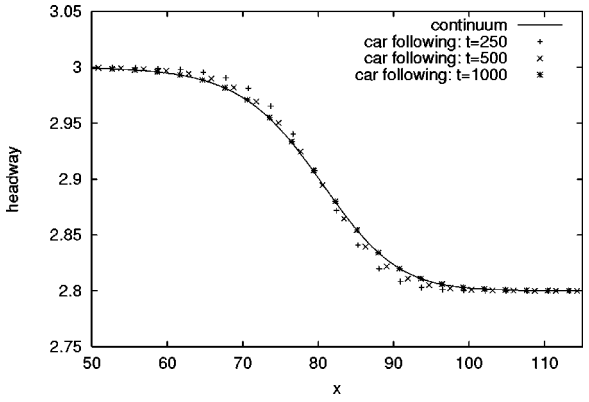

FIG. 2. The shock wave profile of the Bando model approaching the traveling wave solution of the continuum model.

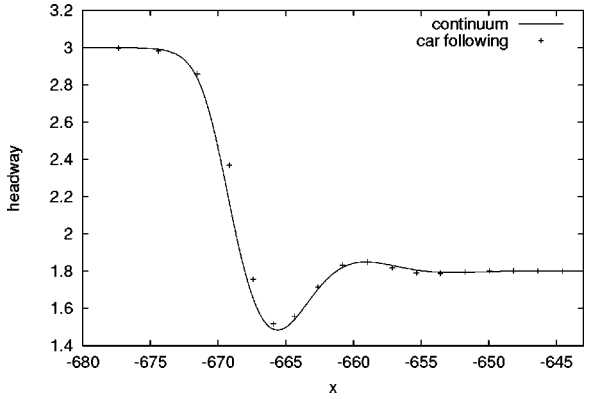

FIG. 3. The change of headway after $t=1000$ for an initial jump from $b_-=3.0$ to $b_+=1.8$.

$$c_{up,down}=\frac{\rho_\pm \overline{V}(\rho_\pm)-\rho_{gap}\overline{V}(\rho_{gap})}{\rho_\pm-\rho_{gap}}. \tag{62}$$

The gapwidth d_{gap} then has the long-time form

$$d_{gap}=v_{gap}(t-t_{initial}),\quad t\gg t_{initial}, \tag{63}$$

where $t_{initial}$ is the time offset associated with the development of the waves. Once more it can only be estimated by numerical solutions of the car-following model and comparison (Figs. 4 and 5) suggests that $t_{initial}\approx -189.78$. For the set of parameters

$$\rho_-=3.0, \tag{64}$$

$$\rho_+=1.7, \tag{65}$$

we find from the numerics the gap density to be

$$\rho_{gap}\approx 1.303 \tag{66}$$

and the gap speed from the continuum model

$$v_{gap}=-0.6597-(-6858)=0.0261. \tag{67}$$

This corresponds very well with the slope of the curve in Fig. 5. We are now able to compare the Bando wave and the two individual traveling wave solutions of the continuum model in the same graph (Fig. 6), which shows a very good

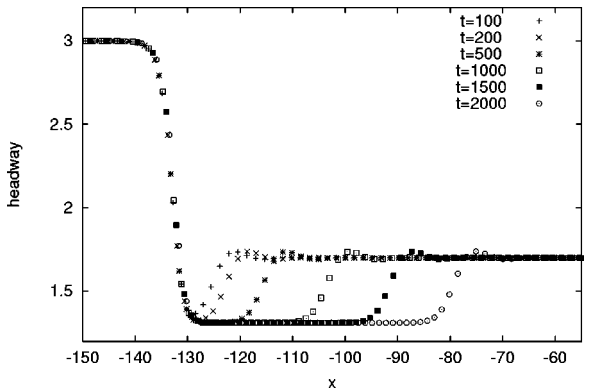

FIG. 4. The forming of a Bando wave for initial values $b_-=3.0$ and $b_+=1.7$.

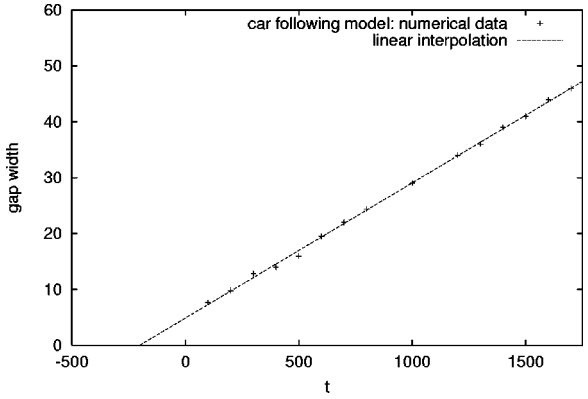

FIG. 5. Determination of the time offset $t_{initial}$ of the Bando wave .

agreement. We conclude that our continuum model is a very good approximation to the discrete car-following Bando model (1).

V. COMPARISON WITH THE KERNER-KONHÄUSER MODEL

Next we show that the transformation (17) is crucial in order to derive a continuum model that is qualitatively analogous to the underlying car-following model. To this end we compare predictions of our model with those of a previously published continuum model and the corresponding car-following model. Herrmann and Kerner [11] investigated the similarities between their continuum model and a car-following model that is also based on a relaxation term. They considered in greater detail cluster effects in both models by examining traffic jams in a Bando type model

$$\dot{v}_n=\frac{1}{T}[V_B(b_n)-v_n] \tag{68}$$

and comparing the predictions to their own continuum model

$$\rho_t+(\rho v)_x=0, \tag{69}$$

$$v_t+vv_x=\frac{1}{T}[V_{kk}(\rho)-v]-c_0^2\frac{\rho_x}{\rho}+\mu\frac{v_{xx}}{\rho}. \tag{70}$$

In both cases they chose the same OV function

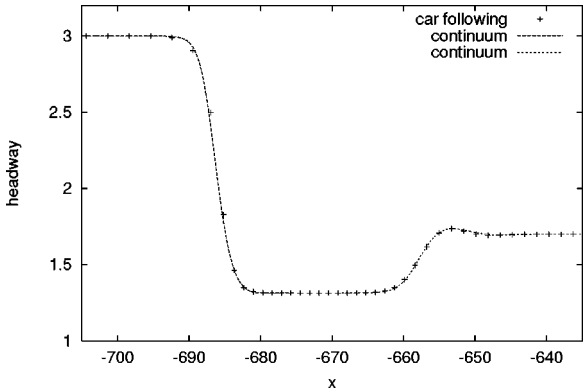

FIG. 6. Comparison of the Bando wave and two individual traveling wave solutions of the continuum model (60).

$$V_{kk}(\rho)=v_0\left[\left(1+\exp\frac{(\rho-\rho_i)/\hat{\rho}}{\sigma}\right)^{-1}-d\right] \tag{71}$$

with

$$d=\left(1+\exp\frac{1-\rho_i/\hat{\rho}}{\sigma}\right)^{-1} \tag{72}$$

and

$$V_B(b)=V_{kk}(1/b). \tag{73}$$

The top speed of cars is defined as $v_f:=V_{kk}(0)$. The parameters of the car-following model are fitted until both models show the same wide stationary jams in their simulations moving on a circular road. This gives the following parameters for the discrete model:

$$T=0.985 \text{ s}, \tag{74}$$

$$\hat{\rho}=180 \text{ vehicles/km}, \tag{75}$$

$$v_f=100.8 \text{ km/h}, \tag{76}$$

$$\rho_i=36.5 \text{ vehicles/km}, \tag{77}$$

$$\sigma=0.02875, \tag{78}$$

whereas the parameters of the continuum model are based on real traffic data:

$$T=5 \text{ s}, \tag{79}$$

$$c_0=39.88 \text{ km/h}, \tag{80}$$

$$\mu=210 \text{ vehicles km/h}, \tag{81}$$

$$\hat{\rho}=180 \text{ vehicles/km}, \tag{82}$$

$$v_f=100.8 \text{ km/h}, \tag{83}$$

$$\rho_i=42.7 \text{ vehicles/km}, \tag{84}$$

$$\sigma=0.04. \tag{85}$$

For unstable flow these two models may seem to describe the same qualitative type of moving structures such as dense-sparse regions. However, if we examine the stable regime, we find that these models are actually not equivalent. For comparison Fig. 7 shows how the Kerner-Konhäuser model cannot match the length scale of a jump in headway of a traveling wave predicted by the car-following model (68). Even for the same driver reaction time $T=0.985$ s the model predicts a much more extensive region of adjustment in order for the headway to decrease to $b=40$ m.

The calculations are carried out by substituting Eq. (53) into Eq. (70) to obtain the traveling wave equation analogous to Eq. (60)

$$uu_z=\frac{1}{T}[V_{kk}(q_0/u)-u-c]+c_0^2\frac{u_z}{u}+\frac{\mu}{q_0}uu_{zz}. \tag{86}$$

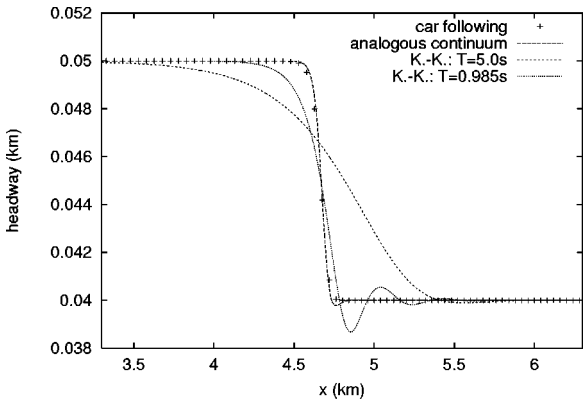

FIG. 7. Comparison of traveling waves in the Bando model (68), the Kerner-Konhäuser (K.-K.) model (86), and the model (60) in the stable region for the same optimal velocity function.

We now compare solutions of this ODE and the car-following model (68) to those of our continuum model (60) with an OV function as in Eq. (73) and parameters as in Eqs. (74)–(78). Our model predicts oscillatory behavior in contrast to the car-following model, but significantly it predicts the same length scale (Fig. 8). This arises from the dependency of the coefficients of the higher order terms on either the density (23) or the velocity (60).

This dependency does not occur in conventional continuum models, but it could well be an intrinsic feature of a delay differential equation as recently proposed by Nagatani [12], [13]. In order to derive a modified Kortweg–de Vries equation for the jamming transition in a continuum model he used a simplified version of the Kerner-Konhäuser model

$$(\rho v)_t=a\rho_0 V(\rho(x+1))-a\rho v \tag{87}$$

with the OV function $V(\rho)=V_B(1/\rho)$ of the Bando model (1). He simplifies it in the sense that he drops the pressure and the dispersive terms of the original model. On the other hand, the anticipation is now incorporated in a nonlocal term $\rho(x+1)$. In this model that is dimensionless in space the average headway b_{av} is supposed to be of order one ($b_{av}=1$). The idea is that a driver adjusts his velocity according to the observed headway $b(x)=1/\rho(x+1)$. Even though this is not the correct relation between headway and density as shown above we proceed to derive the corresponding ordi-

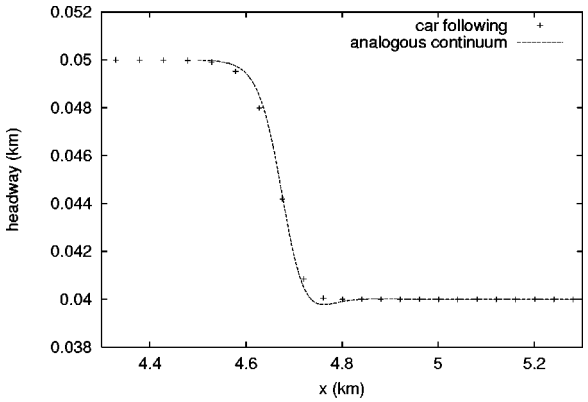

FIG. 8. Comparison of traveling waves in the Bando model (68) and the analogous continuum model (60).

nary differential equation for the traveling waves. Nagatani couples the dynamic equation to a continuity equation of the form

$$\rho_t+\rho_0(\rho v)_x=0. \tag{88}$$

In case of a traveling wave the transformation (50)–(52) enables integration of Eq. (88) to give

$$\rho(\rho_0 v-c)=q_0. \tag{89}$$

Inserting this relation into Eq. (87) yields

$$ww_z=\frac{a\rho_0^2}{q_0c^2}V\left(\frac{q_0}{w(z+1)}\right)w^3-\frac{a}{c^2}w^3-\frac{a}{c}w^2 \tag{90}$$

with

$$w=\rho_0 v-c. \tag{91}$$

Since this is a delay differential equation it is not straightforward to compare it to our model (60). In general a delay differential equation cannot be solved by a Taylor expansion and its truncation after a certain amount of terms. Nevertheless in order to have similar equations the first terms of the Taylor expansion should be similar. If we keep terms up to first order in V'

$$V\left(\frac{q_0}{w(z+1)}\right)\sim V\left(\frac{q_0}{w(z)}\right)-q_0V'\left(\frac{q_0}{w(z)}\right)\frac{w_z(z)}{w(z)^2}-\frac{1}{2}q_0V'\left(\frac{q_0}{w(z)}\right)\left[\frac{w_{zz}(z)}{w(z)^2}-2\frac{w_z^2(z)}{w(z)^3}\right] \tag{92}$$

we obtain a corresponding second order model

$$ww_z=\frac{a\rho_0^2}{q_0c^2}\left[V\left(\frac{q_0}{w}\right)-q_0V'\left(\frac{q_0}{w}\right)\left(\frac{w_z}{w^2}+\frac{w_{zz}}{2w^2}-\frac{w_z^2}{w^3}\right)\right]w^3-\frac{a}{c^2}w^3-\frac{a}{c}w^2 \tag{93}$$

that differs not only by its expansion terms but also by the nonlinear terms aw^3/c^2 and aw^2/c. Hence the class of solutions differs also from our model. Nevertheless the expansion (93) shows that a dependency of the coefficients of the pressure and dispersive terms on the density is an intrinsic feature of this model. But it is not an analogous model of the Bando model.

VI. TRAVELING WAVES IN THE UNSTABLE REGION

The correspondence of the traveling wave solutions of both the continuum and the car-following model cannot be generalized to all values of the sensitivity parameter a. The line

$$l_{\mathrm{SB}}(b)=2V_B'(b) \tag{94}$$

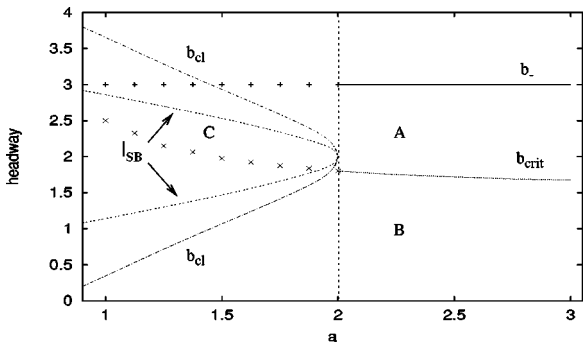

FIG. 9. Traveling waves with upstream $b_-=3$ and downstream headway $b_+=b_{\mathrm{crit}}$ become unstable for $a<2$ and form clusters with headways given by the curve b_{cl}.

defines a region SB in the headway-sensitivity diagram in which the model is linear unstable (Fig. 9). For $a\geqslant 2$ the model is linear stable and the traveling wave solutions with the specific initial condition $b_-=3.0$ and $b_+<b_-$ can be divided into two regions. In region A the traveling wave solutions are linear stable unless the downstream value b_+ hits the critical value b_{crit} when Bando waves form. This type of wave as described above occurs in region B. The two traveling waves with a growing region of a specific headway b_{gap} in between are stable.

Keeping the upstream and downstream headway fixed and varying a, the traveling wave solutions eventually become unstable for sufficiently small values of a. Formally we still obtain solutions from the ODE (60) so that b_{crit} can be derived. But whether a particular solution is stable or unstable depends on the values of the headways which are involved. If the upstream and downstream headways are not part of the region SB and the adjustment does not consist of an oscillatory overshoot that intersects SB, then the solution is linear stable and can be reproduced by the car-following model with corresponding initial conditions as presented above.

On the other hand, the solution is unstable if these conditions are not fulfilled. Figure 10 shows how an initial jump in headway evolves with time in the car-following model. After $t=50$ the solution is very similar to those of the continuous counterpart (60) but eventually it becomes unstable and the typical cluster forms. For given a the solution eventually jumps between two headways. Their values can be read from the graph b_{cl} in Fig. 9.

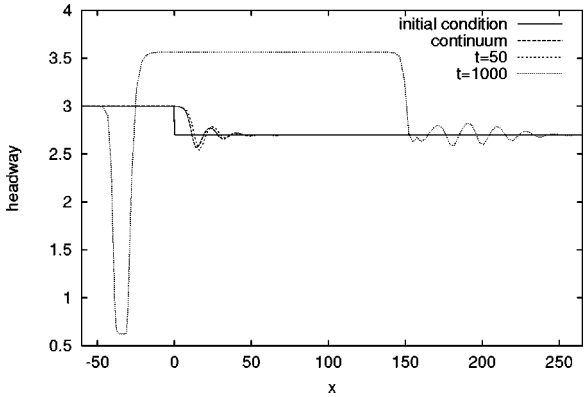

FIG. 10. The traveling wave solution of a modest jump in headway from $b_-=3$ to $b_+=2.7$ in the unstable regime ($a=1.0$) cannot be reproduced by the continuum model. Clusters form.

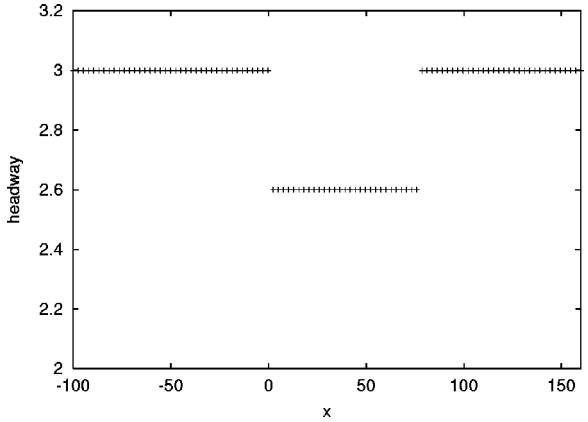

FIG. 11. Initial condition: region of slightly higher congested traffic.

Whether traveling waves of the region C, the corresponding region of A in the unstable regime, are stable or not has to be investigated in every single case. If either the upstream or downstream headway is part of the region SB, then the solution is clearly unstable and develops towards the corresponding cluster solutions. For $b_-=3$ and $b_+ \gtrsim b_{\mathrm{crit}}$ the solutions turn out to be generally unstable for $a<2$.

The rich structure of the stability of traveling waves is part of future research.

VII. ASYMPTOTIC SOLUTIONS

So far we have considered traveling wave solutions of the Bando model, its continuous counterpart, and the Kerner-Konhäuser model. The first two showed a very good agreement for a number of different steady traffic situations. It is also of interest to examine the dynamic case of a nonstationary wave solution. This can be done in certain regimes, because in some special cases the higher order terms of dynamic equations of the form

$$v_t + v v_x = a[V(\rho) - v] + O(\rho_x, \rho_{xx}) \tag{95}$$

do not play an important role and can be neglected. The traffic flow is then uniquely determined by the driver's sensitivity a and the optimal velocity function $V(\rho)$ combined with the equation for the conservation of cars (22).

As an example one might consider an initial disturbance in the (car-following) Bando model (1) as in Fig. 11. Here, a region of slightly higher congested traffic is situated in between a homogeneous flow. As time increases, one ends up with a wave solution shown in Fig. 12. The headway overshoots the initial disturbance by a shock and eventually readjusts to the original headway. The jump in headway decreases with time, and a dispersive tail forms. As can be seen from the graph, there is a ''stationary point'' K_0 along the road, where the solutions intersect until the downstream propagating, nonlinear shock front passes this point.

This effect can be explained in a very simple continuum model, similar to that of Lighthill and Whitham [14], which is based on the conservation of cars by substituting the stationary relation

$$q(\rho) = V(\rho)\rho \tag{96}$$

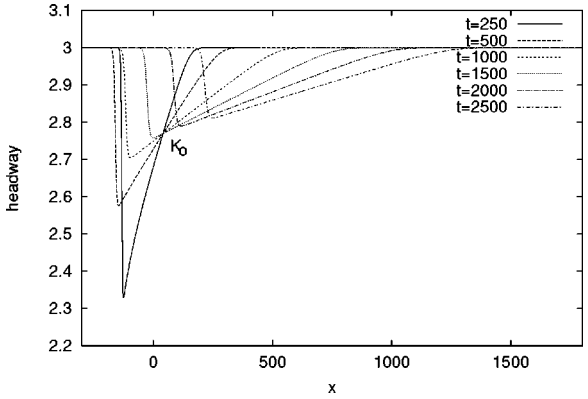

FIG. 12. The evolution of the pulse in Fig. 11.

between the flow and the density for q to obtain

$$\rho_t + q(\rho)_x = 0 \tag{97}$$

$$\Leftrightarrow \rho_t + [V(\rho)\rho]_x = 0. \tag{98}$$

This model does not incorporate inertia. By use of the method of characteristics it turns out that regions of density ρ travel with speed

$$c(\rho) = \frac{\partial q(\rho)}{\partial \rho} = V(\rho) + \rho \frac{\partial V(\rho)}{\partial \rho}, \tag{99}$$

which is equivalent to the slope of the tangent in the fundamental diagram in Fig. 13. K_0 is therefore simply the maximum ρ_0 of this curve, where the speed of the density wave vanishes. To explain the other features, we start with the higher order continuum model (23). First we simplify the wave profile by piecewise linear solutions, which model a triangle evolving in space and time as shown by Fig. 14 (cf. Whitham, [15]). For the dispersive tail one can formally write an asymptotic solution ($t \to \infty$) as

$$\rho(x,t) = \rho_0 + \hat{\rho}(x,t) = \rho_0 + \rho_1 \frac{x^\alpha}{t^\beta}, \ \frac{\hat{\rho}}{\rho_0} \ll 1, \tag{100}$$

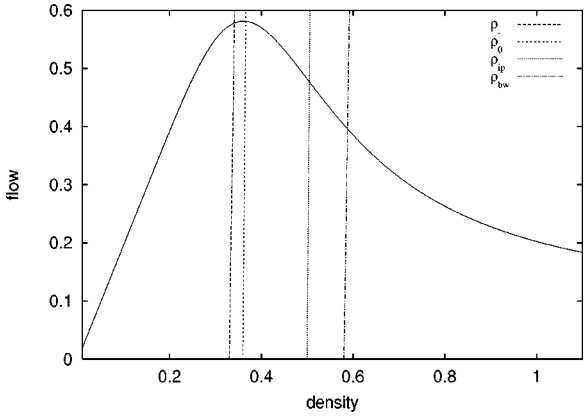

FIG. 13. Fundamental diagram of the Bando model with significant densities: undisturbed density ρ_-, maximum of the flow ρ_0, inflection point ρ_{ip}, and the onset of the Bando wave ρ_{bw}.

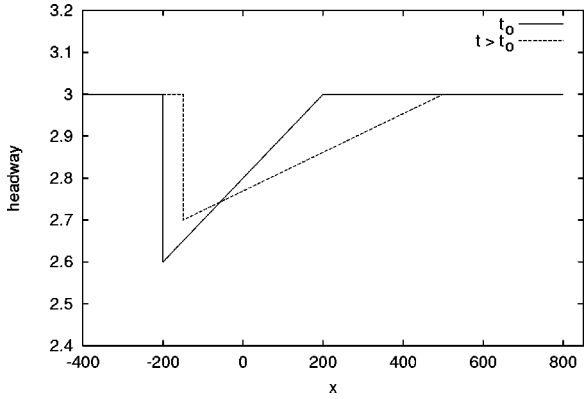

FIG. 14. A model for the pulses.

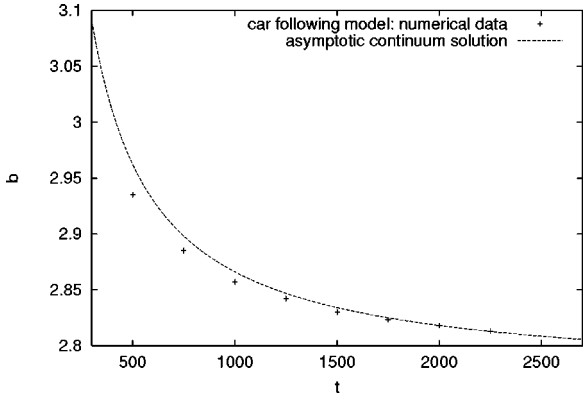

FIG. 15. Comparison of the numerical data and the asymptotic solution (117) at $x=200$.

$$v(x,t)=v_0+\hat{v}(x,t)=v_0+v_1\frac{x^\gamma}{t^\delta},\quad \frac{\hat{v}}{v_0}\ll 1. \tag{101}$$

Two equations have to be balanced. Apart from the conservation of cars, there is also the dynamic equation

$$v_t+vv_x=a[\overline{V}(\rho)-v]+a\overline{V}'(\rho)\left[\frac{\rho_x}{2\rho}+\frac{\rho_{xx}}{6\rho^2}-\frac{\rho_x^2}{2\rho^3}\right]. \tag{102}$$

By substituting Eqs. (100) and (101), it is seen that the relaxation term $a[\overline{V}(\rho)-v]$ dominates all the other terms as $t\to\infty$ and $x\to\infty$, because they incorporate time and space derivatives. Therefore this term has to vanish exactly, leading to

$$v=\overline{V}(\rho), \tag{103}$$

$$\alpha=\gamma, \tag{104}$$

$$\beta=\delta. \tag{105}$$

Equation (103) can be substituted into the conservation of cars (97), which leads to Eq. (98). A Taylor expansion of $\overline{V}(\rho)\rho$ around some value ρ_0

$$\overline{V}(\rho)\rho=(\overline{V}\rho)_0+(\overline{V}\rho)_0'\hat{\rho}+\frac{1}{2}(\overline{V}\rho)_0''\hat{\rho}^2+\cdots \tag{106}$$

(dash equals derivative with respect to ρ) analogous to the asymptotic expansions (100) and (101) gives us

$$\hat{\rho}_t+(\overline{V}\rho)_0'\hat{\rho}_x+(\overline{V}\rho)_0''\hat{\rho}\hat{\rho}_x=0. \tag{107}$$

Near the maximum ρ_0 of the flow, the first derivative vanishes, and a possible balance can be extracted from

$$-\rho_1\beta\frac{x^\alpha}{t^{\beta+1}}+(\overline{V}\rho)_0''\rho_1^2\alpha\frac{x^{2\alpha-1}}{t^{2\beta}}=0 \tag{108}$$

as

$$\alpha=1,\ \beta=1,\ \text{and}\ \ \rho_1=\frac{1}{(\overline{V}\rho)_0''}<0. \tag{109}$$

Now the density around the flow maximum becomes

$$\rho(x,t)=\rho_0+\rho_1\frac{x}{t} \tag{110}$$

$$=0.36-0.062\,\frac{x}{t} \tag{111}$$

and the velocity

$$v=\overline{V}(\rho)\simeq\frac{\overline{V}\rho}{\rho}=\frac{(\overline{V}\rho)_0+(\overline{V}\rho)_0''\hat{\rho}^2}{\rho_0+\hat{\rho}} \tag{112}$$

$$\Rightarrow v(x,t)\simeq\frac{(\overline{V}\rho)_0}{\rho_0}-\frac{(\overline{V}\rho)_0}{\rho_0^2(\overline{V}\rho)_0''}\frac{x}{t} \tag{113}$$

$$=1.61+0.28\,\frac{x}{t}. \tag{114}$$

The headway is given by

$$b(x,t)=b_0+\hat{b}(x,t) \tag{115}$$

$$=\frac{1}{\rho_0}-\frac{\rho_1}{\rho_0^2}\frac{x}{t} \tag{116}$$

$$=2.78+0.48\,\frac{x}{t}. \tag{117}$$

This corresponds to an increasing velocity and headway, respectively, which is consistent with the graph. To compare the asymptotic solution (117) with the numerical data from the car-following model, we place the origin in Fig. 12 at the stationary point K_0 where the pulses intersect and take the data from $x=200$. The dependency on x is obviously linear, but the inverse time relation as well as the coefficient ρ_1 have to be checked. Figure 15 shows a very good agreement between both these data, so that we can regard the tail as been understood. What remains is the movement of the shock. But here one more look onto the fundamental diagram gives a qualitative explanation. Two successive jumps in headway are drawn in Fig. 14. The shock moves with velocity

$$\dot{x} = c(\rho) = \frac{q_- - q(\rho)}{\rho_- - \rho} \tag{118}$$

[cf. Eq. (58)] along the road where ρ denotes the highest density of the pulse. The change of the jump in headway is given by the intersection of the asymptotic solution (111) and the shock front

$$\dot{\rho} = \dot{\hat{\rho}} + \frac{\partial \hat{\rho}}{\partial x} c(\rho) \tag{119}$$

$$= -\frac{x}{(\overline{V}\rho)_0'' t^2} + \frac{1}{(\overline{V}\rho)_0'' t} c(\rho) \tag{120}$$

[where $\dot{\hat{\rho}}$ is the change of the tail and $(\partial\hat{\rho}/\partial x)c(\rho)$ is the change of the shock front]. This system of coupled differential equation describes the motion of the shock along the road. It is easy to see that it must turn around at a point when

$$\dot{x} = c(\rho) = q_- - q(\rho) = 0, \tag{121}$$

and eventually it passes by the stationary point K_0.

The features of traffic flow described in this chapter can be described by a simple continuum model, in which the length scale of evolution of the flow is long compared to $1/a$, the relaxation required by traffic to adjust to the optimal velocity OV. Hence, the flow is accurately modeled by assuming that it has the optimal velocity.

VIII. CONCLUSION AND OUTLOOK

We derived a continuum model from a second-order car-following (Bando) model by using an integral representation of the headway. This enables us to transform the headway and the velocity consistently by using an asymptotic approximation for the headway in terms of the density. For car-following models of the Bando type, including an optimal velocity function V, we gave a general expression of the equivalent continuum model, even though the transformation allows for any model to be transformed into its continuous counterpart. In the case of the Bando model [1] the continuum version obeys the same stability criterion as the discrete counterpart. Numerical simulations of the Bando model predict the formation and evolution of traffic shocks. These are well modeled by traveling waves using our continuum model provided the gradients are moderate.

The transformation to the continuum model delivers a powerful tool for traffic simulations. To calculate the traveling wave solutions on a straight road the programs for the Bando model simulations required about 4 h (2000 cars, stepsize $\Delta t = 0.005$, simulation time $t = 2000$; Pentium 233 MHz) according to 2000 coupled differential equations, whereas the solution of the ODE's (60) or (86) took just about 5 s. In addition the continuum model allows for simple estimations of overall traffic quantities. Some features of the autonomous cruise control systems (ACCS), whose algorithms for the regulation of headway are often based on dynamic equations similar to the Bando type (1), may be investigated in a continuum manner.

ACKNOWLEDGMENTS

P.B. would like to thank the Alfried Krupp von Bohlen und Halbach-Stiftung and the EPSRC for their sponsorships of this project.

[1] M. Bando, K. Hasebe, A. Nakayama, A. Shibata, and Y. Sugiyama, Phys. Rev. E **51**, 1035 (1995).
[2] K. Nakanishi, K. Itoh, Y. Igarashi, and M. Bando, Phys. Rev. E **55**, 6519 (1997).
[3] M. Bando, K. Hasebe, K. Nakanishi, A. Nakayama, A. Shibata, and Y. Sugiyama, Phys. Rev. E **58**, 5429 (1998).
[4] H. Hayakawa and K. Nakanishi, Phys. Rev. E **57**, 3839 (1998).
[5] B.S. Kerner and P. Konhäuser, Phys. Rev. E **50**, 54 (1994).
[6] A. Bachem, M. Schreckenberg, and D.E. Wolf, *Traffic and Granular Flow* (World Scientific, Singapore, 1996).
[7] K. Nagel, Phys. Rev. E **53**, 4655 (1996).
[8] A.D. Mason, Ph.D. thesis, University of Cambridge, 1998 (unpublished).
[9] J. Bevan and A.W. Woods (unpublished).
[10] J. Bevan, master's thesis, University of Bristol, 1998 (unpublished).
[11] M. Herrmann and B.S. Kerner, Physica A **255**, 163 (1998).
[12] T. Nagatani, Physica A **261**, 589 (1998).
[13] T. Nagatani, Physica A **264**, 581 (1999).
[14] M.J. Lighthill and G.B. Whitham, Proc. R. Soc. London, Ser. A **229**, 317 (1955).
[15] G.B. Whitham, *Linear and Nonlinear Waves* (John Wiley & Sons, New York, 1974).